Characterization of layer-by-layer self-assembled carbon nanotube multilayer thin films

Nanotechnology **18** (2007) 145709 (7pp) doi:10.1088/0957-4484/18/14/145709

Characterization of layer-by-layer self-assembled carbon nanotube multilayer thin films

Wei Xue and Tianhong Cui[1]

Department of Mechanical Engineering, University of Minnesota, 111 Church Street SE, Minneapolis, MN 55455, USA

E-mail: tcui@me.umn.edu

Received 4 December 2006, in final form 9 February 2007
Published 6 March 2007
Online at stacks.iop.org/Nano/18/145709

Abstract

Single-walled carbon nanotube (SWNT) multilayer thin films are deposited on silicon substrates with layer-by-layer self-assembly. The structural, mechanical, electrical, and thermal properties of the thin films are investigated using quartz crystal microbalance (QCM), nanoindentation, and rapid thermal annealing techniques, respectively. Scanning electron microscopy inspection shows that the SWNT multilayer is formed through a dense network of nanotube bundles. Based on the QCM measurement, the volume and mass ratios of SWNTs in the multilayer are calculated as 63.2% and 75%, respectively. Nanoindentation on the SWNT thin film shows that its Young's modulus and hardness are approximately 17 and 0.6 GPa, respectively. Current–voltage (I–V) and four-point probe techniques are used to study the electrical properties of the SWNT thin film after being heated at different temperatures. The conductance of the SWNT thin film at 300 °C is measured as 2.29 mS, which is 50 times higher than that at room temperature (0.045 mS).

(Some figures in this article are in colour only in the electronic version)

1. Introduction

Carbon nanotubes (CNTs) have attracted much attention since their discovery in 1991 [1]. CNTs have high mechanical, thermal, and chemical stability as well as high electrical mobility. A CNT is a novel nanoscale material that has outstanding versatility and wide applicability [2]. It can be used as electrical, mechanical, and sensing component in various applications [3–5]. Individual CNT-based devices have been investigated extensively [6, 7]. However, due to the ultra-small dimensions of the CNTs, the difficulty of manipulating individual nanotubes reduces the throughput of the devices. This has become one of the most serious bottlenecks for developing and commercializing CNT-based devices. The process to fabricate individual CNT devices is often time-consuming and complicated. In addition, the controllability and reproducibility of such devices are very low. In contrast, the use of CNT thin films, in the form of an aligned array or random network, can circumvent these problems, and can be a compromise between time/complexity and size. The process of producing CNT thin films is faster, simpler, and has higher yield.

Layer-by-layer (LbL) self-assembly based on electrostatic force can be used to grow highly reproducible CNT thin films. The self-assembly technique provides a simple, low-cost, and low-temperature method to produce CNT thin films. The first CNT thin film fabricated with LbL self-assembly was reported by Mamedov and his co-workers in 2001 [8]. Characterization shows that the self-assembled CNT thin film is uniform and has high mechanical strength. Its ultimate tensile strength can reach up to 325 MPa, close to that of ultrahard ceramics. This technique was quickly adopted by several groups for building CNT/polymer multilayer thin films. Both single-walled and multi-walled carbon nanotube (SWNT and MWNT) thin films were successfully assembled on silicon substrates [9, 10]. The CNTs in the assembled

[1] Author to whom any correspondence should be addressed.

thin films normally retain their electrochemical catalytic activities and can be used for chemical and biosensing applications. Amperometric sensors based on self-assembled CNT thin films were developed for sensing H_2O_2, choline, and dopamine [11–13]. Furthermore, a biocompatibility study showed that it is possible to develop implantable devices based on self-assembled polyelectrolyte/CNT thin films [14].

In this paper, we report the characterization of SWNT multilayer thin films fabricated with LbL self-assembly. The films are built with alternating layers of negatively charged SWNTs and positively charged polyelectrolyte–poly(dimethyldiallylammonium chloride) (PDDA). The growth of the SWNT thin film can be controlled in the nanometre scale. The structural, mechanical, electrical, and thermal properties of the assembled SWNT thin films are investigated by various equipment, including a quartz crystal microbalance (QCM), nanoindentation tester, four-point probe, and rapid thermal annealer (RTA). The characterization results are described and discussed.

2. Experiment

SWNTs (produced with the chemical vapour deposition method, average diameter: 1.1 nm, average length: 50 μm, density: 2.1 g cm^{-3}, purity >90%) were purchased from Chengdu Organic Chemical Co., Ltd. To increase the solubility, the pristine SWNTs were chemically functionalized by a mixture of nitric and sulfuric acid (1:3 HNO_3:H_2SO_4) at 110 °C for 45 min. After the acid treatment, the SWNTs were negatively charged by covalently attached carboxylic (–COOH) groups on the sidewalls and the open ends; the SWNTs were uniformly dispersed in deionized (DI) water with a concentration of approximately 1 mg ml^{-1}. In addition to the purpose of chemical functionalization, the nitric acid is used to purify the pristine SWNTs by etching away the amorphous carbon and other impurities [15, 16]. The polyelectrolytes including PDDA (molecular weight 200 000–350 000, polycation) and poly(sodium 4-styrenesulfonate) (PSS, molecular weight 70 000, polyanion) were obtained from Sigma-Aldrich. The PDDA and PSS were diluted in DI water with concentrations of 15 and 3 mg ml^{-1}, respectively. The pH values of PDDA and PSS were measured as 7.5 and 6.5, respectively. In order to increase the ionic strength and enhance the adsorption of the polyions, 0.5 M NaCl was added to both polyelectrolyte solutions.

Recently, we reported a technique to pattern SWNT multilayer two-dimensional (2D) microstructures and three-dimensional (3D) cantilever arrays [17]. The simple and effective technique combines LbL self-assembly, microlithography, and lift-off techniques by using positive photoresist as the sacrificial layer. The SWNT multilayer is built through submerging the substrate in alternating solutions. The sequence of the immersion is: [PDDA (10 min) + PSS (10 min)]$_2$ + [PDDA (10 min) + SWNTs (15 min)]$_n$, where n represents the number of (PDDA/SWNT) bilayers [18]. The entire assembly process is carried out at room temperature, approximately 24 °C.

The structure of the self-assembled SWNT multilayer thin film is shown in figure 1(a). The assembled SWNT multilayer was inspected by a high-resolution scanning

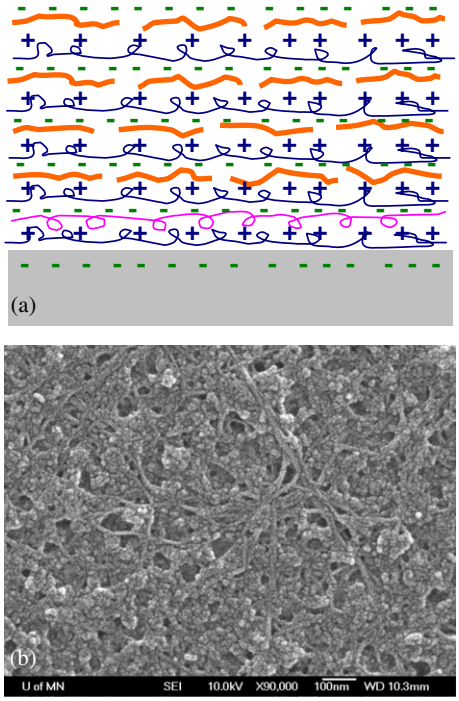

Figure 1. (a) Structure of self-assembled SWNT multilayer thin film on Si substrate. (b) SEM image of assembled SWNTs. The sample contains five (PDDA/SWNT) bilayers.

electron microscope (SEM, JEOL 6500). The SEM image allows close observation of the assembled SWNTs on the substrate. As shown in figure 1(b), the SWNT multilayer is formed by a dense network of SWNTs. The SWNTs are randomly deposited on the substrate. The lengths of the SWNTs are in the range of 1–2 μm because of the shortening process of the chemical functionalization. However, it is difficult to estimate the diameters of the assembled SWNTs from the SEM image. The SEM used for inspection has an ultimate resolution of 1.5 nm, and it is difficult to distinguish individual SWNTs (diameter: 1.1 nm) in the SEM image. However, a great number of SWNTs can be seen in the image. The reason is that several SWNTs are wrapped together and form nanotube bundles in the SWNT dispersion due to their extremely high aspect ratios. The diameters of the nanotube bundles are at least several times larger than those of the individual SWNTs. To obtain a reasonable estimation of the SWNT bundle diameters, a quartz crystal microbalance (QCM, Maxtek RQCM) was used.

3. Results and discussion

3.1. Structural characterization

The QCM technique was used to monitor the assembling process by detecting the mass changes of a sensing crystal. The QCM equipment is an extremely sensitive sensor capable of detecting mass changes in the ng cm^{-2} range. It also provides real-time measurement of crystal frequency and frequency shift. Therefore, the saturation time for adsorbing polyelectrolytes and SWNTs can be estimated. The

measurements were carried out at room temperature. An AT cut, (the most popular thickness-shear crystal unit fabricated today) 9 MHz, 1 inch diameter crystal with Au electrodes was used as the sensing crystal due to its superior mechanical and piezoelectric properties. The crystal was held vertically in the solutions to avoid excessive adsorption of polyelectrolytes and SWNTs. First, the crystal was soaked in PDDA and PSS several times to pre-charge the Au electrodes. Afterwards, the crystal was immersed in a PDDA solution and SWNT dispersion for given periods of time. At the same time, the real-time frequency shift of the crystal was recorded by the QCM. The mass change ΔM (g) and the frequency shift Δf (Hz) can be expressed by the Sauerbrey equation [19]:

$$\Delta f = -C_f \times \Delta m = -C_f \times \frac{\Delta M}{A} \tag{1}$$

where $C_f = 1.81 \times 10^8$ (Hz cm^{-2} ng^{-1}) is the sensitivity factor of the 9 MHz AT cut crystal, Δm (g cm^{-2}) is the change in mass per unit area, $A = 0.34$ cm^2 is the active oscillation region of the crystal which is limited to the overlapping area of the front and rear Au electrodes. Therefore, 1 Hz change in frequency corresponds to 1.88 ng change in mass. The Sauerbrey equation can also be expressed as

$$d = -\frac{\Delta f}{\rho \cdot C_f} \tag{2}$$

where d is the layer thickness, ρ is density of the deposited material, ρ_{PDDA} is 1.2 g cm^{-3}, and ρ_{SWNT} is 2.1 g cm^{-3} [20].

Figure 2 shows the growth of a (PDDA/SWNT)$_6$ multilayer monitored with the QCM. The left y-axis shows the recorded frequency shift Δf and the right y-axis illustrates the calculated layer thickness. The average frequency changes of PDDA and SWNTs are -61.1 and -182.5 Hz, respectively. Based on (2), the calculated layer thicknesses for PDDA and SWNT are $d_{\mathrm{PDDA}} = 2.8$ nm and $d_{\mathrm{SWNT}} = 4.8$ nm, respectively. Therefore, the thickness of a (PDDA/SWNT) bilayer is approximately 7.6 nm. The volume and mass ratios of SWNTs in the multilayer can be calculated as

$$\frac{V_{\mathrm{SWNT}}}{V} = \frac{d_{\mathrm{SWNT}} \cdot A}{(d_{\mathrm{SWNT}} + d_{\mathrm{PDDA}}) \cdot A} = 63.2\% \tag{3}$$

$$\frac{m_{\mathrm{SWNT}}}{m} = \frac{\rho_{\mathrm{SWNT}} \cdot d_{\mathrm{SWNT}} \cdot A}{\rho_{\mathrm{SWNT}} \cdot d_{\mathrm{SWNT}} \cdot A + \rho_{\mathrm{PDDA}} \cdot d_{\mathrm{PDDA}} \cdot A} = 75\%. \tag{4}$$

As a whole, the density of a (PDDA/SWNT) bilayer $\rho = 1.77$ g cm^{-3} can be obtained by substituting the frequency shift $\Delta f = -243.6$ Hz and $d = 7.6$ nm into (2).

We presented another two methods to measure the thickness of (PDDA/SWNT)$_n$ multilayer in our early report [17]. The multilayer was measured mechanically by a surface profiler and optically by an ellipsometer. The average thickness of a (PDDA/SWNT) bilayer was approximately 75.9 Å, which is very close to the value obtained by the QCM technique.

3.2. Mechanical characterization

The mechanical properties of LbL self-assembled SWNT multilayer thin films were studied as bulk films by Mamedov *et al* [8]. In their experiments, free-standing SWNT films were stretched with a thin-film tensile strength tester, and the stress (σ) versus strain (ε) data were recorded. From the σ–ε curve shown in their report, the Young's modulus of the SWNT thin film is between 17 and 35 GPa. Here we report an alternative approach to detect the mechanical properties of SWNT multilayer thin films. Films with 40 (PDDA/SWNT) bilayers were assembled on silicon substrates. The relatively large number of SWNT layers increases the film thickness and minimizes the influence from the silicon substrates. As coating/substrate systems, the SWNT thin films and the silicon substrates were measured with the nanoindentation technique. The indentation test has been used in industry for material assessment and quality control for decades. A number of mechanical properties such as Young's modulus, hardness, elastic–plastic deformation behaviour, scratch resistance, film-substrate adhesion, residual stresses, time-dependent creep and relaxation properties, fracture toughness, and fatigue can be obtained using commercial or specialized indenters [21]. In the past 20 years, due to the fast development of nanotechnology, the mechanical properties of nanoscale materials have been studied intensively. One important advantage of nanoindentation is that many mechanical properties (such as Young's modulus and hardness) of the coating/substrate system can be extracted from the load–displacement curve, and direct measurement of the produced impressions is not necessary [22]. In a nanoindentation test, the multilayer hardness H, the mean pressure the material can resist, can be calculated as [23]

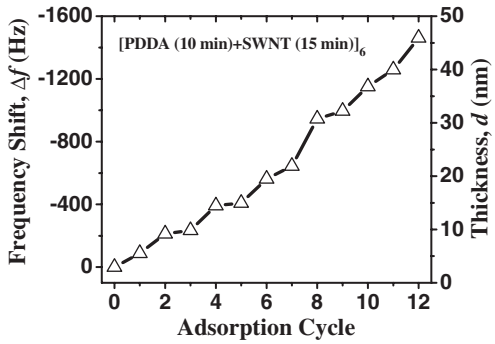

Figure 2. Frequency shift Δf measured with the QCM and corresponding layer thickness calculated from the Sauerbrey equation.

$$H = \frac{P_{\max}}{A_{\mathrm{r}}} \tag{5}$$

where $P_{\max}$ is the maximum indentation load and A_{r} is the residual indentation area. The Young's modulus of the multilayer can be calculated from the following equations:

$$\frac{1}{E_{\mathrm{eff}}} = \frac{(1-v^2)}{E} + \frac{(1-v_i^2)}{E_i} \tag{6}$$

$$S = \frac{\mathrm{d}P}{\mathrm{d}h} = \frac{2}{\sqrt{\pi}} E_{\mathrm{eff}} \sqrt{A} \tag{7}$$

where E_{eff} is defined as the effective Young's modulus, E and v are Young's modulus and Poisson's ratio for the SWNT

multilayer, $E_i = 1141$ GPa and $v_i = 0.07$ are the same parameters for the diamond tip indenter [24], S is the slope of the unloading curve at the maximum load, and A is the projected contact area. If the indentation depth and the shape of the tip indenter are known, the projected contact area A can be calculated accordingly. The Young's modulus can therefore be derived by measuring the unloading curve slope at the maximum load.

A commercially available depth-sensing nanoindentation tester (NanoIndenter XP, MTS) was used to characterize the mechanical properties of the SWNT multilayer thin films. A dynamic indentation technique called continuous stiffness measurement (CSM) developed by Oliver and Pharr was used in the indentation tests [23]. During the CSM process, a small amplitude oscillation with relatively high frequency is superimposed on the dc indenter-load control signal. Physically, a three-sided pyramid indenter tip is driven perpendicularly into, then out of, the film, as shown in figure 3(a). The thicknesses of the $(PDDA/SWNT)_{40}$ multilayer thin films on the silicon substrates are approximately 300 nm, estimated from the structural characterization described above. The Young's modulus of the silicon substrate is 170 GPa. To minimize the influence from the substrates, the indentation depth limits on the SWNT thin films were set as 80 nm (or 26.7% of the film thickness).

The recorded load–displacement curves for three samples are shown in figure 3(b). All three samples exhibit similar behaviour under indentation loading and unloading processes. The actual indentation depths are 65–70 nm (or 23.3% of the film thickness) and the maximum loads are 0.14–0.18 mN. The Young's moduli of the SWNT thin films extracted from the load–displacement data are shown in figure 3(c). From the figure, the Young's moduli decrease first, and start to increase after 10 nm. The extracted values from the first 10 nm are not accurate because the tip may slip away from the SWNT or may indent between adjacent SWNTs during the indentation process. After 10 nm, the tip indents inside the SWNT thin films and the extracted values are more accurate. At higher depth, however, the substrate starts to have effects on the indentation process. For nanoindentation tests on coating/substrate systems, the measured coating properties are considered to be independent of the substrate properties when the indentation depth is no greater than 10% of the coating thickness [22]. At 30 nm (or 10% of the SWNT multilayer thickness), the moduli for all three samples are approximately 17 GPa, close to the results measured by Mamedov *et al* [8]. The extracted hardness values of the SWNT thin films are shown in figure 3(d). The hardness, as a function of depth, shows a sharp decline followed by a gradual increase. The initial hardness reflects the presence of SWNTs on the surface, which is what the tip indenter is in contact with initially. At 30 nm, the hardness is approximately 0.6 GPa. Compared with strong polymers which are commonly used in MEMS devices such as poly(methyl methacrylate) (PMMA, Young's modulus: 2 GPa), an SWNT multilayer is several times stronger. An SWNT multilayer also has enough flexibility due to its composite essence. In general, SWNT multilayer thin films have mechanical properties between those of silicon and polymers. Therefore, they can serve as structural components in MEMS devices to provide both flexibility and strength.

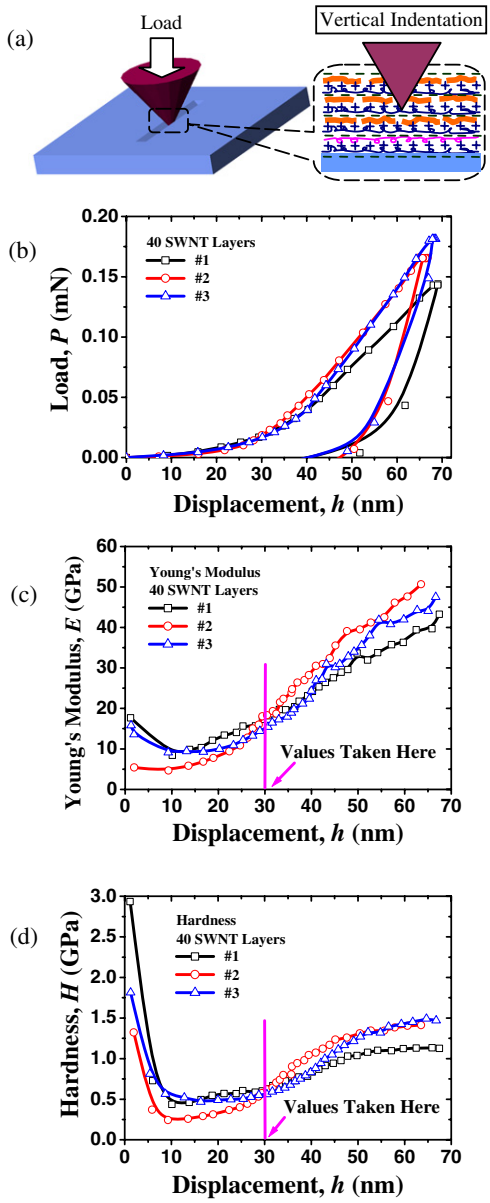

Figure 3. (a) Scheme of nanoindentation test on assembled SWNT multilayer thin films, (b) load–displacement curves, (c) measured Young's moduli, and (d) hardness of $(PDDA/SWNT)_{40}$ multilayer thin films on silicon substrates.

3.3. Electrical and thermal characterization

In order to study the electrical and thermal properties of SWNT multilayer thin films, a number of SWNT thin film resistors were fabricated on Si/SiO_2 substrates. Figure 4 shows the schematic structure and the cross-sectional SEM image of the resistor. Metal layers of Cr/Au (1000 Å/2000 Å) were electron-beam evaporated on the substrate and patterned as electrode pads. The Cr layer was used to enhance the adhesion between the Au layer and the substrate. Afterwards, a thin film composed of a $(PDDA/SWNT)_{16}$ multilayer was self-assembled on the substrate as a resistor. The width w and the length l of the resistor were 1 and 6 mm, respectively. The resistors were characterized using an HP 4156A semiconductor parameter analyser. The resistance can be calculated from

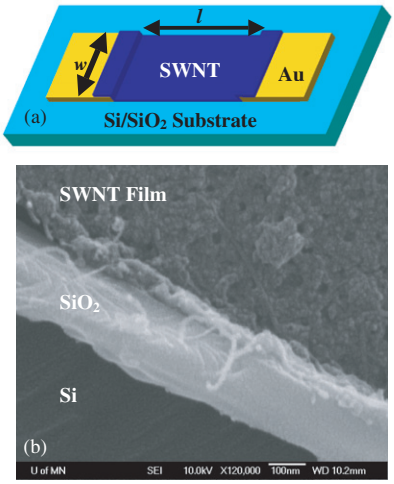

Figure 4. (a) Schematic structure of an SWNT thin-film resistor. (b) Cross-sectional SEM image of Si/SiO_2 substrate and SWNT thin film.

the measured current–voltage (I–V) curves. The scan range of the applied voltage was set as −1.5 to 1.5 V with a step of 10 mV. However, the results obtained from the I–V technique are often affected by lead and contact resistances introduced by the equipment. In order to verify the results obtained from I–V characterization, the resistivity of the $(PDDA/SWNT)_{16}$ multilayer was also measured with the four-point probe technique. The four-point probe equipment (Veeco FPP 5000) has four equally spaced probes in line. A dc current passes through the outer two probes and the voltage is measured between the inner two probes. This technique solves the problem of added lead and contact resistances that exists in I–V technique. Therefore, more accurate results can be obtained. The temperature dependence of the electrical properties of the SWNT multilayer was studied by heating the device in a rapid thermal annealer (RTA, Modular Process Technology RTP-600S) at different temperatures ranging from 100 to 700 °C. At each temperature, the sample was heated for 1 min. The ambient gas used in the process contained 10% O_2 and 90% N_2; the flow rate was set as 8 SLPM (standard litres per minute).

The electrical properties of the thermally annealed SWNT resistors and multilayer thin films were characterized with both I–V and four-point probe techniques. Figure 5 shows three measured I–V curves at room temperature 24 °C, after samples were treated at 300 °C and 600 °C for 1 min with the RTA. All curves demonstrate highly linear properties in the range of −1.5 to 1.5 V. This implies that the semiconducting SWNTs inside the thin film work in the linear I–V region. In addition, the metallic SWNTs are interconnected and form a highly conductive channel due to the dense SWNT network fabricated with LbL self-assembly.

The conductance G at different temperatures T calculated from the I–V curves is illustrated in figure 6(a). The inset figure shows the resistance R calculated from the same data. The conductance increases first when the temperature is raised from room temperature (0.045 mS) to 200 °C (0.085 mS). A dramatic change happens at 300 °C: the conductance increases by approximately 27 times, from 0.085 mS (at 200 °C) to

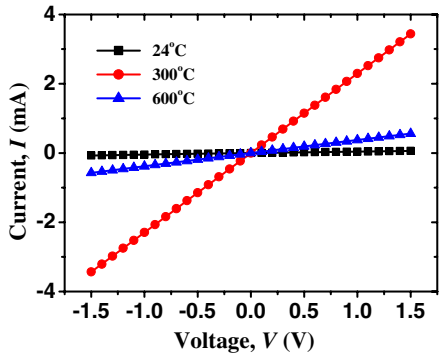

Figure 5. Current–voltage (I–V) curves of an SWNT thin-film resistor annealed at different temperatures.

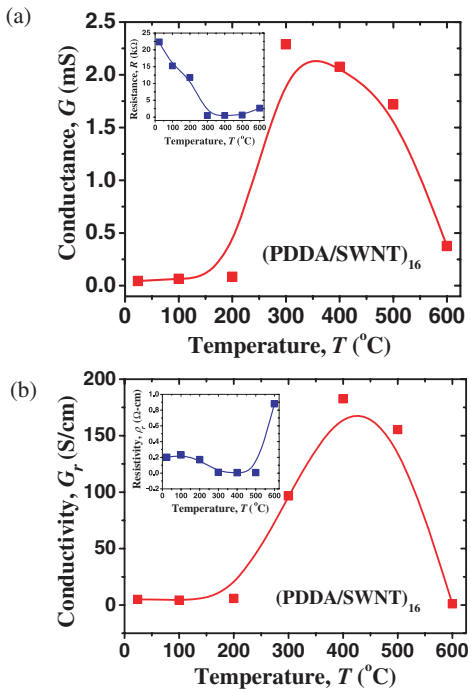

Figure 6. Electrical–thermal study of the SWNT thin film. (a) The conductance G (inset: resistance R) obtained from current–voltage (I–V) characterization. (b) Conductivity G_r (inset: resistivity ρ_r) obtained from the four-point probe measurement.

2.29 mS (at 300 °C). After 300 °C, the conductance slowly decreases to approximately 0.38 mS (at 600 °C). The SWNT thin-film resistor was measured as an open circuit after being heated at 700 °C for 1 min. The four-point probe technique was used to verify the observed electrical–thermal behaviour by measuring the resistivity ρ_r (in Ω cm) of the SWNT thin film directly. The measured conductivity G_r(in S cm^{-1}) = $1/\rho_r$ at different temperatures from the four-point probe is shown in figure 6(b) and the resistivity ρ_r is illustrated in the inset. The G_r–T curve is very similar to the G–T curve shown in figure 6(a). The G_r value changes dramatically from 5.87 (at 200 °C) to 96.62 S cm^{-1} (at 300 °C). In contrast to the I–V characterization, the highest G_r = 182.61 S cm^{-1} occurs at 400 °C. This difference comes from the measurement methods. For I–V characterization, the measured location is

determined by the pre-patterned Au electrodes. However, for the four-point probe test, the measured location varies each time. The variation of the location introduces uncertainties of the measured results. When the SWNT thin film was heated at 700 °C for 1 min, an 'out-of-range' value was observed.

The electrical–thermal behaviour of the SWNT thin film can be divided into three parts with PDDA as the main cause. The SWNT layers in the film are separated by the intermediate PDDA layers due to the fabrication process. PDDA is composed of carbon, hydrogen, nitrogen, and chloride with the C:H:N:Cl ratio 8:12:1:1. At high temperatures, the hydrogen and nitrogen components of PDDA are able to react with oxygen and produce H_2O and N_xO_y, respectively. When the temperature is lower than 200 °C, the PDDA in the SWNT multilayer is partly consumed by oxygen. The PDDA layers become thinner, leading to a better connection between the separated SWNT layers. Most PDDA molecules are able to keep their natural forms and hold the multilayer together. Therefore, the conductance of the SWNT multilayer increases slightly. When the temperature increases from 200 to 500 °C, more hydrogen and nitrogen components of the PDDA are consumed, and a large portion of the PDDA molecules is carbonized. The SWNTs and the carbonized PDDA molecules are interconnected, which leads to the dramatic increase of the film conductance. At temperatures higher than 600 °C, most hydrogen and nitrogen components of the PDDA are consumed and evaporated, and most PDDA molecules are carbonized. The PDDA layers lose their electric charges and cannot hold the multilayer together. As a result, the SWNT multilayer is easily blown off from the substrate by the gas flow in the RTA chamber. There are almost no SWNTs left on the substrate at temperatures higher than 700 °C.

4. Conclusion

SWNT multilayer thin films have been successfully fabricated with a 'bottom-up' LbL self-assembly process. The assembly technique provides a simple, low-cost, and low-temperature fabrication method to produce ultrathin films with a short processing time. The assembled SWNT thin films have been characterized using several techniques. The structural, mechanical, electrical, and thermal properties of the SWNT thin films have been studied. The SWNT multilayer thin films have mechanical properties between those of silicon and hard polymers. Both flexibility and strength can be provided by the SWNT multilayer thin films. Highly linear I–V characteristics are observed from the SWNT thin-film-based resistors. The conductance of the SWNT multilayer can be adjusted in a wide range by annealing the device at different temperatures. Further research, especially the study of electrochemical properties and biosensing characteristics, needs to be done to gain a thorough understanding of LbL self-assembled SWNT multilayers. SWNTs multilayer thin films can be used in a number of applications due to their unique and outstanding properties. They can serve as various components in NEMS/MEMS, microelectronic devices, and biosensors. The controllability, reliability, and flexibility of the deposition technique provide us with great opportunities for the development of practical SWNT thin-film devices.

Acknowledgments

This work is partially supported by DARPA MEMS/NEMS Fundamental Research Program through the MF3 Center. We thank the Nanofabrication Center at the University of Minnesota for the help in micro/nanofabrication. We also thank Dr Xun Yu for helpful discussion about the material preparation.

References

[1] Iijima S 1991 Helical microtubules of graphitic carbon *Nature* **354** 56
[2] Chen R J, Choi H C, Bangsaruntip S, Yenilmez E, Tang X, Wang Q, Chang Y and Dai H 2004 An investigation of the mechanism of electronic sensing of protein adsorption on carbon nanotube devices *J. Am. Chem. Soc.* **126** 1563–8
[3] Bradley K, Gabriel J P, Star A and Grüner G 2003 Short-channel effects in contact-passivated nanotube chemical sensors *Appl. Phys. Lett.* **83** 3821–3
[4] Xu Z, Chen X, Qu X, Jia J and Dong S 2004 Single-wall carbon nanotube-based voltammetric sensor and biosensor *Biosens. Bioelectron.* **20** 579–84
[5] Xue W, Liu Y and Cui T 2006 High-mobility transistors based on nanoassembled carbon nanotube semiconducting layer and SiO_2 nanoparticle dielectric layer *Appl. Phys. Lett.* **89** 163512
[6] Li S, He P, Dong J, Guo Z and Dai L 2005 DNA-directed self-assembling of carbon nanotubes *J. Am. Chem. Soc.* **127** 14–5
[7] Besteman K, Lee J, Wiertz F G M, Heering H A and Dekker C 2003 Enzyme-coated carbon nanotubes as single-molecule biosensors *Nano Lett.* **3** 727–30
[8] Mamedov A A, Kotov N A, Prato M, Guldi D M, Wicksted J P and Hirsch A 2002 Molecular design of strong single-wall carbon nanotube/polyelectrolyte multilayer composites *Nat. Mater.* **1** 190–4
[9] Rouse J H and Lillehei P T 2003 Electrostatic assembly of polymer/single walled carbon nanotube multilayer films *Nano Lett.* **3** 59–62
[10] Zhang M, Yan Y, Gong K, Mao L, Guo Z and Chen Y 2004 Electrostatic layer-by-layer assembled carbon nanotube multilayer film and its electrocatalytic activity for O_2 reduction *Langmuir* **20** 8781–5
[11] Zhang M, Gong K, Zhang H and Mao L 2005 Layer-by-layer assembled carbon nanotubes for selective determination of dopamine in the presence of ascorbic acid *Biosens. Bioelectron.* **20** 1270–6
[12] Lan Y, Wang E, Song Y, Kang Z, Jiang M, Gao L, Lian S, Wu D, Xu L and Li Z 2005 Covalent assembly of shortened multiwall carbon nanotubes on polyelectrolyte films and relevant electrochemistry study *J. Colloids Interface Sci.* **284** 216–21
[13] Qu F, Yang M, Jiang J, Shen G and Yu Q 2005 Amperometric biosensor for choline based on layer-by-layer assembled functionalized carbon nanotube and polyaniline multilayer film *Anal. Biochem.* **344** 108–14
[14] Gheith M K, Sinani V A, Wicksted R L, Matts R L and Kotov N A 2005 Single-walled carbon nanotube polyelectrolyte multilayers and freestanding films as a biocompatible platform for neuroprosthetic implants *Adv. Mater.* **17** 2663–70
[15] Liu J *et al* 1998 Fullerene pipes *Science* **280** 1253–6
[16] Rinzler A G *et al* 1998 Large-scale purification of single-wall carbon nanotubes: process, product, and characterization *Appl. Phys.* A **67** 29–37
[17] Xue W and Cui T 2006 Carbon nanotube micropatterns and cantilever arrays fabricated with layer-by-layer nano

self-assembly *Sensors Actuators* A (*Preprint* doi:10.1016/j.sna.2006.10.006) at press

[18] Xue W and Cui T 2007 Deposition and characterization of layer-by-layer nano self-assembled carbon nanotube multilayer thin films *IEEE Int. Conf. on Nano/Micro Engineered and Molecular Systems (Bangkok, Thailand, Jan. 2007)*

[19] Sauerbrey G 1959 Use of crystal oscillators for weighing thin films and for microweighing *Z. Phys.* **155** 206–22

[20] Lvov Y, Ariga K, Onda M, Ichinose I and Kunitake T 1997 Alternate assembly of ordered multilayers of SiO_2 and other nanoparticles and polyions *Langmuir* **13** 6195–203

[21] Bhushan B and Li X 2003 Nanomechanical characterisation of solid surfaces and thin films *Int. Mater. Rev.* **48** 125–63

[22] Bull S J 2005 Nanoindentation of coating *J. Phys. D: Appl. Phys.* **38** R393–413

[23] Oliver W C and Pharr G M 1992 An improved technique for determining hardness and elastic modulus using load and displacement sensing indentation experiments *J. Mater. Res.* **7** 1564–83

[24] Simmons G and Wang H 1971 *Single Crystal Elastic Constants and Calculated Aggregate Properties: A Handbook* (Cambridge, MA: MIT Press)